EACS 2016 – 6th European Conference on Structural Control Sheffield, England: 11-13 July 2016
Paper No. 199

A FLUID INERTER WITH VARIABLE INERTANCE PROPERTIES

Smith, N. D. J.[1] & Wagg, D. J.[1]

[1]Department of Mechanical Engineering, University of Sheffield, Sheffield, S1 3JD, UK.

David.Wagg@sheffield.ac.uk

ABSTRACT. The inerter is a novel dynamic device that is the subject of substantial research interest as a passive vibration control device. In this paper we present results from the design and testing of a novel type of fluid inerter system where the inertance can be varied. This variable inertance is achieved by having a fluid filled cylinder that induces flow in a helical pipe system. The parameters of the helical pipe system can be adjusted to give different amounts of inertial force depending on the requirements. Tests were carried out on the inerter system, and it was shown that with the maximum inertance set-up for this system, the sensitivity of output force to input velocity was approximately 500N force for a 1Hz increase in excitation frequency.

KEYWORDS: Fluid inerter, passive control, experimental tests.

1 INTRODUCTION

The inerter is a novel dynamic device that is the subject of substantial research interest in both academia and industry. The device allows for improved passive control of dynamic systems, such as automotive suspensions, and more recently applications in civil engineering structures. This paper describes the development of an experimental inerter system based on a fluid filled cylinder that induces flow in a helical pipe system. The design allows for different levels of inertance to be selected, and results show good agreement with previously published results.

The inerter concept was first introduced by Smith [1] using the force-current analogy between mechanical and electrical networks. In this context, the inerter is considered to represent the equivalent of the capacitor. As a result it has the property that the force generated is proportional to the relative acceleration between its end points (or nodes). The constant of proportionality for the inerter is called inertance and is measured in kilograms.

One of the first applications for the inerter was in Formula 1 racing car suspension systems, under the name of the J-damper [2]. Since then, the inerter's application in the field of vibration isolation has become much wider. There are several types of inerters: the rack and pinion inerter [1], the ball screw inerter [2], the fluid inerter [3], and the electromagnetic inerter [16]. Applications include vehicle suspensions systems [4, 5, 6, 10, 12], train suspension systems [11], and more recently civil engineering systems [18, 19, 15]. The optimal performance of inerter-based vibration isolation systems has been considered by several authors, see for example [7, 8, 9, 17]. In general inertance is fixed, but some recent devices have investigated the idea of variable inertance [13].

Fluid inerters have the advantage of minimal moving parts, with the inertia effect being generated by the motion of the fluid. This inertial effect has two main ways of being realised. It is either due to the

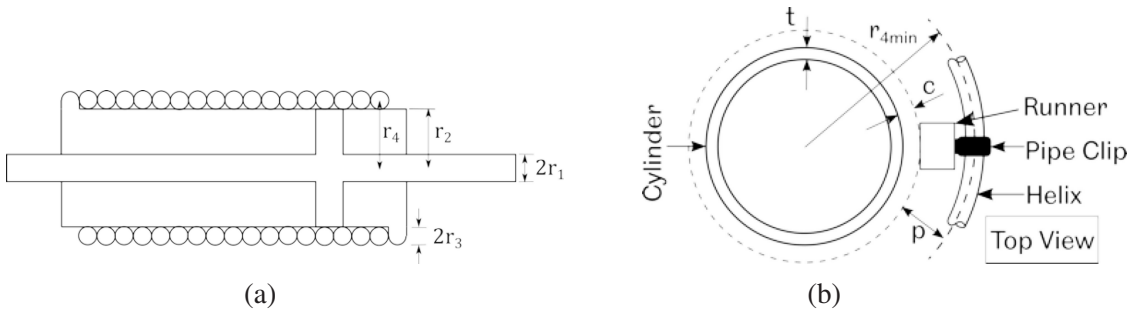

(a) (b)

Figure 1: Helical inerter dimensions

fluid driving a mechanical flywheel (which we denote as the *hydraulic* inerter) or the mass of the fluid itself moving in a helical pipe, which we denote the *helical* inerter. The most recent inerter system is an electromagnetic (EM) variant, for example the device discussed in [16]. In this paper we will describe the testing of a *helical* inerter.

2 DESIGN OF A HELICAL INERTER

A schematic diagram of the helical fluid interter is shown in Figure 1. It should be noted that the helix is external to the main fluid cylinder, as shown in longitudinal cross-section in Figure 1(a). The radius of the main fluid chamber is given by r_2. The piston rod which pushes the fluid inside the main chamber has radius r_1. The distance r_4 is the helix radius from the centre of the longitudinal axis of the cylinder. Other helix parameters are r_3 which is the inner radius of the helical pipe cross-section, h is the pitch of the helix, and n is the number of turns in the helix. Finally L_a is the inner length of the cylinder.

From the definitions above, it follows that the cross-sectional area of the cylinder is $A_1 = \pi(r_2^2 - r_1^2)$ and the cross-sectional area of the helix is $A_2 = \pi r_3^2$. The principal of conservation of mass is applied to derive an expression equating a linear (relative) displacement in the cylinder, x to an angular displacement of a fluid element in the helix, θ. Taking the mass of the liquid in the helix as m_{hel}, then the moment of inertia about the axis of the piston is defined as $J = m_{hel} r_4^2$. If the device is ideal then it is assumed that $\frac{1}{2} b \dot{x}^2 = \frac{1}{2} J \dot{\theta}^2$ where θ is the rotation angle of a particle of fluid in the helix, $\dot{x}$ is the relative velocity between the end points of the inerter, and b is the inertance. These definitions can be used to derive the following expression

$$b = \frac{m_{hel}}{(1 + (h/(2\pi r_4))^2)} \left(\frac{A_1}{A_2}\right)^2, \tag{1}$$

which gives a relationship between the helix radius, r_4 and inertance, b [14]. As a result, by changing r_4, different values of b can be achieved (although not during operation of the inerter). This type of variable radius is implemented on our inerter design by using a system of adjustable pipe clips attached to the runners combined with flexible tubing for the helical pipe, as shown schematically in Figure 1(b).

To determine damping, the mean velocity of the fluid in the helix u, the pressure drop Δp and liquid viscosity μ are used. The Reynolds number Re for pipe flow is defined for laminar flow as $Re = 2 \times 10^3$. The helix mean flow velocity is taken from the Hagen-Poiseuille formula for flow in a straight pipe, $u = (r_3^2 \Delta p)/8\mu L$, where L is the helix pipe length. This allows the laminar damping force F_{dp}^l to be calculated, where superscript l denotes laminar flow.

For turbulent flow, a smooth pipe is considered and Darcey's formula is used to find the pressure drop. The damping force for turbulent flow is F_{dp}^t, where superscript t denotes turbulent flow. These values are taken from the formulas

$$F_{dp}^l = \frac{\Delta p A_1}{\dot{x}} = \left(\frac{A_1}{A_2}\right)^2 8\pi\mu L\dot{x} \quad \text{and} \quad F_{dp}^t = 0.664\mu^{0.25}\rho^{0.75}\frac{LA_1}{r_3^{1.25}}\left(\frac{A_1}{A_2}\right)^{1.75}\dot{x}^{1.75}. \tag{2}$$

2.1 Design of experimental inerter

The inerter was designed to produce an inertance between 5-100kg. The other requirement was that the inerter should have approximately 100mm stroke. Therefore, the formulae above were used to select the appropriate components to build the experimental inerter system.

The inerter was built using an steel cylinder with end-plates (flanges) at either end, into which slots were machined radially (perpendicular to the cylinder axis). Runner rods were then aligned parallel to the cylinder body and retained within the slots. The helix was formed from 12mm (internal diameter) flexible tubing, constrained by pipe clips which slide up and down the runners. Movement of the runners, within the machined slots, provided the required radial helix adjustment while axial movement of the pipe clips also provided pitch adjustment. This can be seen more clearly in Figure 1(b). The oil used inside the inerter was Mobil Velocite No. 3 which has a dynamic viscosity of 0.00168Pas at 40°C and density of 802kg/m^3. A T-ported valve allowed the inerter to be primed (filled) with oil and then switched into an operating mode.

2.2 Testing set-up

The completed inerter installed in the test rig is shown in Figure 2. The test rig is a hydraulic test machine that can be used to give a dynamic displacement signal to the inerter. The lower part of the inerter is constrained and connected to a force transducer. The upper part is attached to a hydraulic actuator, the position of which is measured with a linear variable differential transformer (LVDT). The actuator is controlled using computer software. A laser thermometer was used to monitor the inerter temperature to ensure a consistent operating temperature.

Experimental parameters were in the range to r_{4max}= 120mm, r_{4min}= 30mm, and the nominal set to r_{4min}=80mm. The minimum pitch is a tight helix (each coil touching its neighbour) where the pitch is approximately $2r_3$, ignoring the tube wall thickness. Maximum pitch would be a single coil implying, $h \approx L_a$. The nominal n value was 5.5 turns. These parameters were used to create three different helix configurations for testing, and these are shown in Figure 3. Details of the specific set-up parameters for each test phase are given in Table 1. Also included in Table 1 is a predicted inertance value based on Equation (1). From this we see that Phases 0 & 1 are very low inertance, Phase 2 is maximum for our

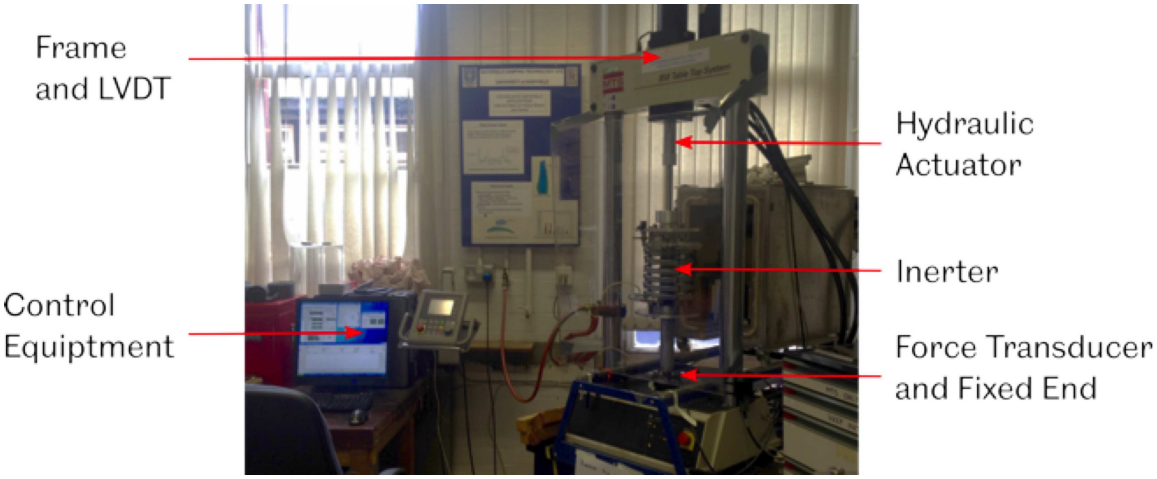

Figure 2: Labelled photograph of the experimental set-up

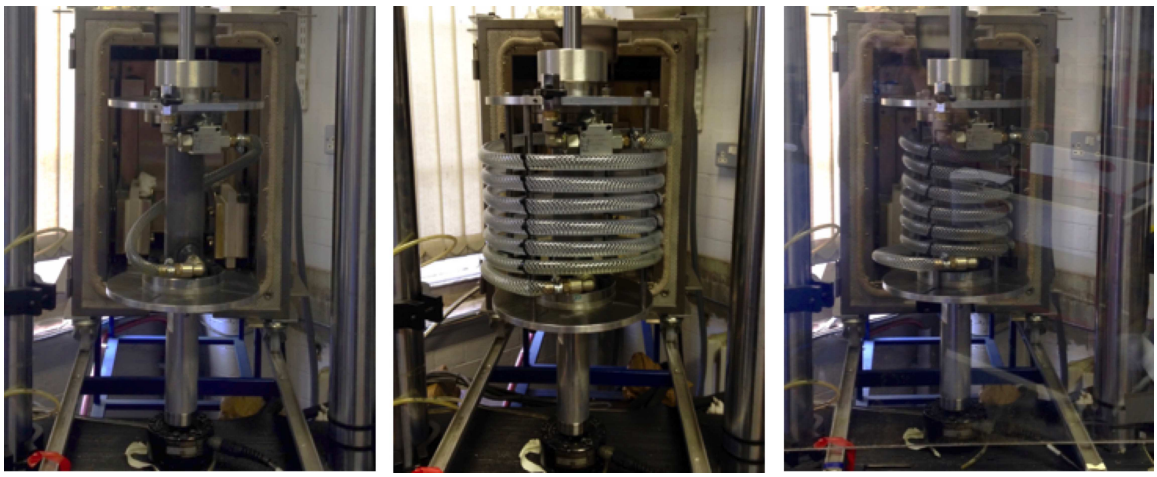

Figure 3: Inerter set-ups for phase 0&1 (left), phase 2 (centre) and phase 3 (right)

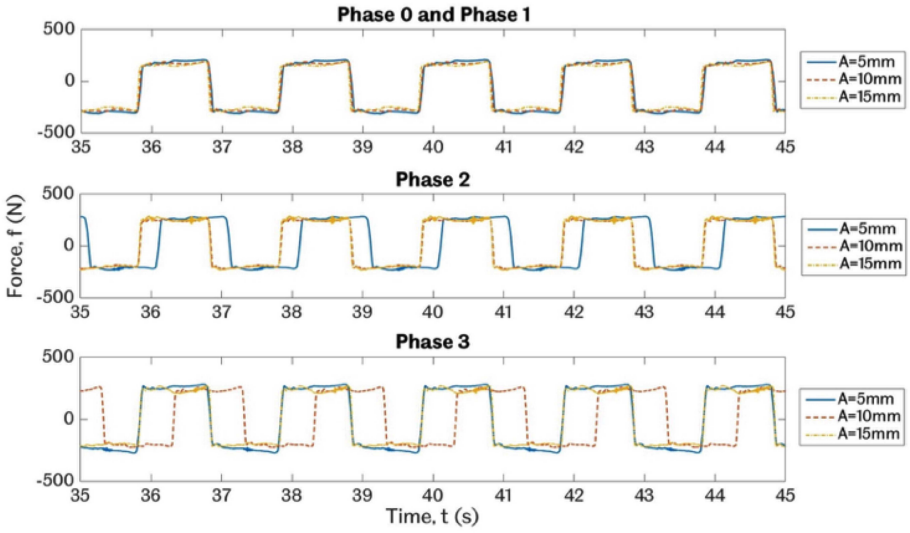

Figure 4: Force response to a sinusoidal displacement input for each test phase at frequency 0.5Hz and amplitude 5-15mm. The differences in signal phase should be ignored, this is due to the piston having a different start position at the beginning of each test.

experimental inerter (because it is the smallest h and largest r_4 for this rig), and Phase 3 is a intermediate value.

Table 1 Test phase set-ups

Test Phase	h (mm)	r_4 (mm)	Frequency range (Hz)	Predicted inertance (kg)
0	190	60	0.2–2	5.8
1	190	60	0.5–10	5.8
2	30	120	0.5–10	75.9
3	30	80	0.5–10	49

3 RESULTS

In this section we will show a sample of the results obtained from the testing carried out. At low frequency values the velocity was very low, and as a result dynamic effects were much less significant. To test this low velocity behaviour, a periodic sine wave input was applied to the three different test phase set-ups, using a low frequency of 0.5Hz and three amplitude values in the range 5-15mm. The results are shown in Figure 4 from which it can be seen that in all cases dynamic effects are minimal, even for Phase 2 where inertance is maximised. This is because of the low velocity input, meaning that the response is dominated by friction effects (mainly mechanical friction of the seals).

As the excitation speed increased, dynamic effects were observed, as the fluid in the helix began to generate significant inertial force. For example, in Figure 5 we show the force for a Test Phase 2

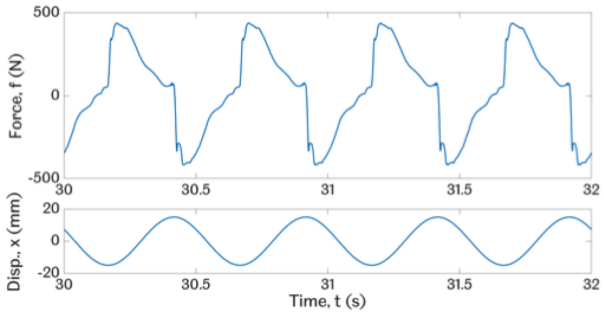

Figure 5: Force response for the phase 2 setup with a sinusoidal displacement input of frequency 2Hz and amplitude 15mm

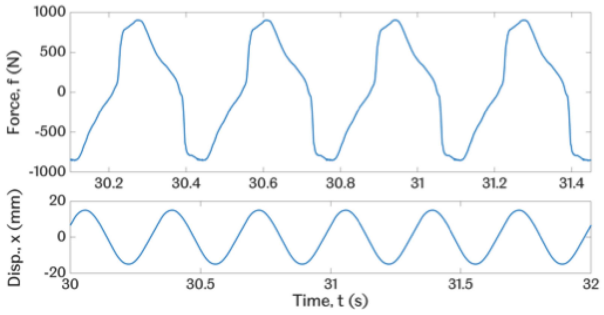

Figure 6: Force response for the phase 2 setup with a sinusoidal displacement input of frequency 3Hz and amplitude 15mm

(maximum inertance) at a frequency of 2Hz and amplitude 15mm with sinusoidal input signal. Now, the force response is dominated by the inertance generated in the helix, and reaching a maximum value of just under 500N. Increasing the input velocity even further shows a very rapid increase in the dynamic effects from the inerter. This can be seen in Figure 6 where the frequency from the previous test result has been increased by just 1Hz, from 2Hz to 3Hz, but the force from the inerter almost doubles to just under 1000N.

4 CONCLUSIONS

In this paper we have presented the results of the design and testing of a novel type of fluid inerter system where the inertance can be varied. This is achieved by having an external helix which can be adjusted to give a required inertial force. Tests were carried out on the inerter system, and it was shown that with the maximum inertance set-up (Phase 2), the sensitivity of output force to input velocity could be made to be approximately 500N increase for a 1Hz increase in input frequency.

In terms of comparison to previous work, the time domain force responses look similar to those

obtained by Swift et al. [20]. The forces observed in low speed tests were (as expected) effectively independent of velocity and dominated by the friction effects inherent in this type of mechanical system.

In terms of designing a helical inerter, these results provide experimental confirmation that minimising h and maximising r_4 will maximise b. In addition the ratio A_1/r_3 must be reasonably high as it strongly influences the available inertance. There were two other factors that affect the performance of the inerter, and these were (i) fluctuating fluid volume and (ii) cavitation. These effects will be considered in detail in future work.

ACKNOWLEDGEMENTS

The authors would like to acknowledge the contribution of the technical support staff from the Department of Mechanical Engineering at the University of Sheffield. In particular thanks to Les Morton, Dave Webster and Ian Hammond for there assistance with the manufacturing, commissioning and testing of the inerter system.

REFERENCES

[1] Smith, M. C. Synthesis of Mechanical Networks: The Inerter. *IEEE Transactions on Automatic Control* 2002; **47**:1648-1662.

[2] Chen, M. Z. Q., Papageorgiou, C., Scheibe, F., Wang, F-C. & Smith, M. C. The missing mechanical circuit. *IEEE Circuits and Systems Magazine* 2009; **1531-636X**:10-26.

[3] Wang, F-C., Hong, M-F. & Lin, T-C. Designing and testing a hydraulic inerter. *Proceedings of the Institution of Mechanical Engineers, Part C: Journal of mechanical Engineering Science* 2010, **225**:66-72.

[4] Papageorgiou, C. & Smith, M. C. Laboratory experimental testing of inerters. *44th IEEE Conference on Decision and Control and the European Control Conference*. Seville, Spain 2005; 3351-3356.

[5] Papageorgiou, C., Houghton, N. E., & Smith, M. C. Experimental Testing and Analysis of Inerter Devices. *Journal of Dynamic Systems, Measurement and Control, ASME* 2009; **131**::011001-1 - 011001-11.

[6] Kuznetsov, A., Mammadov, M., Sultan, I., & Hajilarov, E. Optimization of improved suspension system with inerter device of the quarter-car model in vibration analysis. *Arch. Applied Mechanics* 2011; **81**:1427-1437.

[7] Scheibe, F. & Smith, M. C., Analytical solutions for optimal ride comfort and tyre grip for passive vehicle suspensions. *Journal of Vehicle System Dynamics* 2009; **47**:1229-1252.

[8] Smith, M. C. & Wang, F-C. Performance benefits in passive vehicle suspensions employing inerters. *Journal of Vehicle System Dynamics* 2004; **42**:235-257.

[9] Wang, F-C. & Su, W-J. Impact of inerter nonlinearities on vehicle suspension control. *International Journal of Vehicle Mechanics and Mobility* 2008, **46**:575-595.

[10] Wang, F-C. & Chan, H-A. Vehicle suspensions with a mechatronic network strut. *International Journal of Vehicle Mechanics and Mobility*, Vol. 49, No. 5, 811-830, 2011.

[11] Wang, F-C., Liao, M-K., Liao, B-H., Su, W-J., & Chan, H-A. The performance improvements of train suspension systems with mechanical networks employing inerters. *International Journal of Vehicle Mechanics and Mobility*, Vol. 47, 805-830, 2009.

[12] Evangelou, S., Limebeer, D. J. N., Sharp, R. S., & Smith, M. C. Mechanical steering compensators for high-performance motorcycles. *Transactions of the ASME*, Vol. 74, 332-346, 2007.

[13] Brzeski, P., Kapitaniak, T. & Perlikowski, P. Novel type of tuned mass damper with inerter which enables changes of inertance. *Journal of Sound and Vibration*, 349:56–66, 2015.

[14] Gartner, B. J. & Smith M. C. Damping and inertial hydraulic device, February 7 2011. US Patent App. 13/577,234.

[15] Giaralis, A. & Taflanidis, A. A. Reliability-based design of tuned mass-damper-inerter (tmdi) equipped multi-storey frame buildings under seismic excitation. In *Proc. of 12th International Conference on Applications of Statistics and Probability in Civil Engineering, ICASP12*, 2015.

[16] Gonzalez-Buelga, A., Clare, L. R., Neild, S. A., Jiang, J. Z. & Inman, D. J. An electromagnetic inerter-based vibration suppression device. *Smart Materials and Structures*, 24(5):055015, 2015.

[17] Krenk, S. & Høgsberg, J. Tuned resonant mass or inerter-based absorbers: unified calibration with quasi-dynamic flexibility and inertia correction. In *Proc. R. Soc. A*, volume 472, page 20150718. The Royal Society, 2016.

[18] Lazar, I. F., Neild, S. A., & Wagg, D. J. Using an inerter-based device for structural vibration suppression. *Eathquake Engineering & Structural Dynamics*, 43(8):1129–1147, 2014. DOI: 10.1002/eqe.2390.

[19] Lazar, I. F., Neild, S. A., & Wagg, D. J. Vibration suppression of cables using tuned inerter dampers. *Engineering Structures*, 122:62–71, 2016.

[20] Swift, S. J., Smith, M. C, Glover, A. R. Papageorgiou, C., Gartner, B. & Houghton, N. E. Design and modelling of a fluid inerter. *International Journal of Control*, 86(11):2035–2051, 2013.